Theoretical and Applied Fracture Mechanics 114 (2021) 103004

Contents lists available at ScienceDirect

Theoretical and Applied Fracture Mechanics

journal homepage: www.elsevier.com/locate/tafmec

Compact crack arrest testing and analysis of EH47 shipbuilding steel

Jessica Taylor [a,b], Ali Mehmanparast [a,*], Rob Kulka [c], Philippa Moore [c], Gholam Hossein Farrahi [a,d], Li Xu [e]

[a] Offshore Renewable Energy Engineering Centre, Cranfield University, Cranfield, Bedfordshire MK43 0AL, UK
[b] NSIRC, TWI Ltd, Granta Park, Great Abington, Cambridge CB21 6AL, UK
[c] TWI, Granta Park, Cambridge CB21 6AL, UK
[d] School of Mechanical Engineering, Sharif University of Technology, Tehran, Iran
[e] Lloyd's Register, Global Technology Centre, Southampton SO16 7QF, UK

ARTICLE INFO

Keywords:
Brittle crack arrest
Shipbuilding steel
CCA
Compact crack arrest testing

ABSTRACT

It is vitally important to measure the brittle crack arrest properties of shipbuilding steels to ensure that accidental damage will not result in total structural failure. Wide-plate test methods allow for direct measurement of the crack arrest toughness but this kind of testing is incredibly expensive. Therefore, there is a need for cheaper and simpler test methods which are able to measure a material's brittle crack arrest toughness. In this work, Compact Crack Arrest (CCA) testing, which is standardised in ASTM E1221, has been successfully used to measure the crack arrest toughness of thick sections of EH47 shipbuilding steel. The results from this study have been compared to small-scale test methods. It was found that instrumented Charpy testing gives an overprediction of the CCA results, and nil-ductility transition temperature (NDTT) from Pellini tests gives a conservative estimate. The results presented in this study are discussed in terms of the effectiveness of the CCA test method for measurement of brittle crack arrest toughness and integrity assessment of large-scale structures.

1. Introduction

The issues associated with brittle fracture of shipbuilding steels were first brought to light by the premature failure of some of the Liberty ships during WWII[1]. In modern days, the requirements for shipbuilding steels are set by the International Association of Classification Societies (IACS), which includes assurance organisations worldwide. There is a drive to reduce carbon emissions of the shipping industry by using larger ships which can carry more cargo per journey[2]. These ships require stronger and thicker plates of steel for their hulls, and this carries with it an increased risk of brittle fracture, particularly in the case of bad weather or accidental damage[3,4]. A brittle crack can be prevented from causing catastrophic failure of the structure by ensuring that the materials used have a sufficient resistance to a propagating fracture i.e. high brittle crack arrest toughness[5].

The first standard which was developed for measurement of brittle crack arrest toughness was ASTM E1221:1988[6], which utilises relatively large-scale Compact Crack Arrest (CCA) test specimens. In recent years, the most common method to measure brittle crack arrest toughness is using wide-plate testing [7–17] such as ESSO tests or double-tension tests which have been incorporated into International Standard ISO 20064:2019[18]. It has been shown in previous studies that CCA testing gives a lower-bound approximation to the brittle crack arrest toughness, K_{Ia}, whereas wide-plate testing usually enables the crack arrest toughness, K_{ca}, to be directly measured[19]. Due to the experimental difficulties involved in CCA testing, there has been a limited amount of published results available in the public domain using this test method. The restricted amount of CCA test data which are publicly available in the literature are entirely limited to specimens with thicknesses of below 50 mm[20–24]. Some researchers noted that it was difficult to obtain valid results from this test method and there was high scatter in the test data, which is why wide-plate methods are generally preferred[14,22,25].

Although wide-plate test methods are more likely to give a better prediction of brittle crack arrest toughness, there are many advantages to using CCA testing. Primarily, CCA testing is much cheaper than wide-plate testing. CCA testing requires less extensive instrumentation and set-up of the test; for example it is usually done isothermally rather than under a temperature gradient. Additionally, due to the smaller size and use of wedge loading, there is a lower force requirement for the test machine. For these reasons, it is of interest to carry out CCA tests on

* Corresponding author.
E-mail address: a.mehmanparast@cranfield.ac.uk (A. Mehmanparast).

https://doi.org/10.1016/j.tafmec.2021.103004
Received 2 April 2021; Received in revised form 26 April 2021; Accepted 27 April 2021
Available online 30 April 2021

Nomenclature

a	Crack length
a_0	Initial crack length before test
a_a	Arrested crack length
B	Thickness of the CCA test specimen
B_N	Net thickness between side-grooves
D	Diameter of wedge loading hole
E	Elastic Young's modulus
H	Height of the CCA test specimen
K	Stress intensity factor
K_0	Crack initiation toughness
K_a	Crack arrest toughness
K_{ca}	Crack arrest toughness: critical stress intensity factor for crack arrest under mode I fracture mechanics loading condition
K_{Ia}	Crack arrest toughness: measured via ASTM E1221
L	Length from loading hole to CMOD measurement location
N	Slot width in CCA test specimen
S	Side-groove depth (on each side) in CCA test specimen
T	Temperature
T_{4kN}	Reference Temperature at which a material's arrest force during instrumented Charpy test is 4kN
T_{KIa}	Reference temperature at which a material's arrest toughness is 100MPam^{½}
W	Width of the CCA test specimen
Y	Shape factor
δ	Experimental crack mouth opening displacement
σ_{UTS}	Ultimate tensile strength
σ_{Ys}	Static Yield Strength
σ_{Yd}	Dynamic Yield Strength
CCA	Compact crack arrest
CMOD	Crack Mouth Opening Displacement
EDM	Electrical discharge machining
NDTT	Nil Ductility Transition Temperature

modern shipbuilding steels to determine their viability, with the aim of reducing the cost of brittle crack arrest testing.

In this paper, CCA testing was carried out on 80 mm thick EH47 shipbuilding steel to measure the brittle crack arrest toughness over a range of temperatures. The results from this study provide a unique set of data on relatively large thickness plates using the CCA test method. The obtained results have been compared to predictions of the crack arrest toughness from small-scale testing which are reported in previous research conducted by the authors [26]. These predictions rely on determination of reference temperatures and are based on the master curve approach. The specimen preparation, test procedure, experimental challenges, and the analysis of the test data have been comprehensively explained and are discussed in the following sections.

2. Compact crack arrest test methodology

The experimental studies in this work were carried out on EH47 shipbuilding steel, supplied by Lloyd's Register, which is widely used in industrial applications. EH47 steel was chosen due to the fact that it has been well characterised by other researchers which enables the CCA results obtained from this study to be compared to wide-plate test results available from other researchers' works[16,27]. The mechanical and fracture behaviour of the supplied EH47 steel employed in this study was characterised using small-scale mechanical testing by the authors in a previous publication[26]. The main material properties including the upper shelf Charpy energy, room temperature yield strength, σ_{Ys}, and ultimate tensile strength, σ_{UTS}, the nil-ductility transition temperature (NDTT), and average grain size are summarised in Table 1.

Compact crack arrest testing was carried out in accordance with ASTM E1221[6] on 80 mm thick EH47 shipbuilding steel plates. In total, eight specimens were prepared and tested in this study, denoted CCA1–8. The CCA specimens consisted of full-thickness pieces of material which had a notched slot machined into them. The notch was opened using a wedge load through the hole in the specimen to initiate a brittle crack within a brittle weld bead deposited at the base of the notch.

The predictions of crack arrest toughness using small-scale tests, which were made in the previous paper[26], have been compared against the results from CCA test data obtained from the present study.

3. Specimen design

The mechanical properties of the material, shown in Table 1, were used to choose appropriate specimen dimensions which would meet the strict criteria given in the ASTM E1221 standard[6] and give the best chance of calculating K_{Ia}. The key specimen dimensions are summarised in Table 2 and schematically shown in Fig. 1. As seen in Table 2, all eight specimens had the thickness of $B = 80$ mm, width of $W = 260$ mm, height of $H = 156$ mm, wedge loading hole diameter of $D = 50.8$ mm, length from loading hole to the crack mouth opening displacement (CMOD) measurement location of $L = 65$ mm, slot width of $N = 8.28$ mm, and initial crack length of $a_0 = 55$ mm. Also included in Table 2 are the normalised dimensions for each parameter with respect to the width of the specimen, X/W. According to the guidelines provided in ASTM E1221 standard[6], the thickness, B, of CCA test specimens must be sufficiently large to satisfy plane strain conditions, with the width of the test specimen, W, within the range of $2B \leq W \leq 8B$; and the height, H, is 0.6 W.

In order to make the best use of the available material, it was decided to use a B/W ratio of 0.31, which gives a width of $W = 260$ mm for the plates with the thickness of $B = 80$ mm. The initial normalised crack length, a_0/W, was kept very low to increase the stress intensity around the crack tip and facilitate brittle crack initiation. It was also decided to use an a_0/W of just over 0.2 which is at the lower end of the allowed range recommended by the ASTM E1221 standard[6]. As seen in Fig. 1, all test specimens were side-grooved following the recommendation in

Table 1
Material properties for EH47 shipbuilding steel employed in this study.

Upper shelf Charpy energy (J)	Yield strength (MPa)	Ultimate tensile strength (MPa)	Nil-ductility transition temperature (°C)	Average grain size (μm)
297	490	622	−50	4.1

Table 2
CCA specimen dimensions.

	Dimension (mm)	Ratio to width, X/W
B	80	0.31
W	260	1.00
H	156	0.60
D	50.8	0.20
L	65	0.24
N	8.28	0.03
B_N	60	0.23
S	10	0.04
a_0	55	0.21

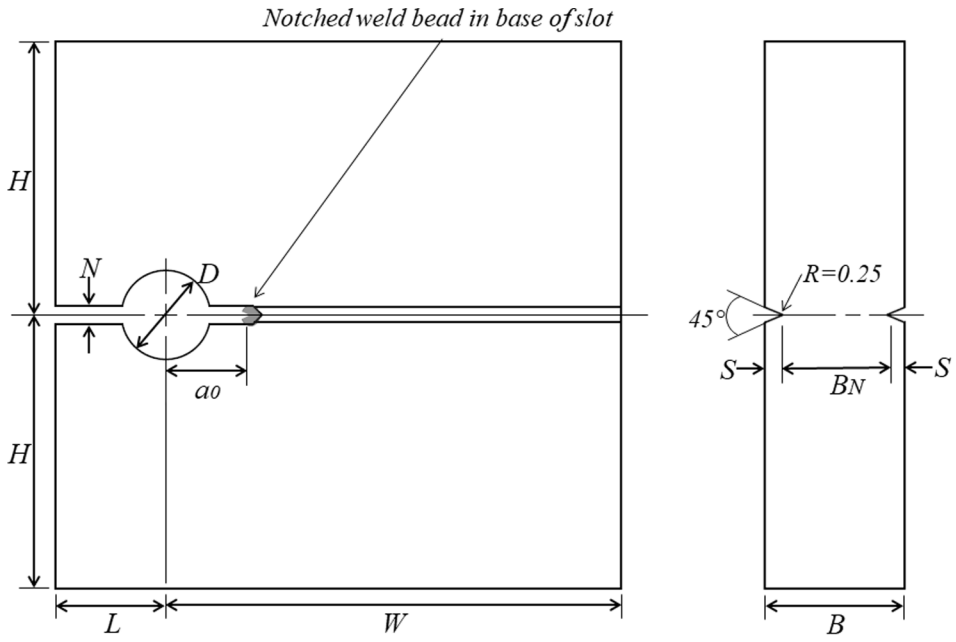

Fig. 1. Schematic illustration of the CCA test specimen design.

the ASTM E1221 standard[6]. Six out of eight specimens were side-grooved on both sides to promote a straight crack front. The remaining two specimens were side-grooved only on one face so that crack propagation monitoring wires could be soldered to the other face of the specimen to measure the crack speed as it propagated. As shown in Table 2, the side-groove depth of $S = 10$ mm was implemented on each side of the test specimens with the net thickness between side grooves of $B_N = 60$ mm in those six specimens with double side-grooves, and $B_N = 70$ mm in those with a single side-groove. As shown in Fig. 1, the test specimens were side-grooved at a 45° angle using an Electrical Discharge Machining (EDM) technique.

4. Introduction of weld beads

A brittle weld bead was laid in the bottom of the slot to give an embrittled material in the starter notch to facilitate brittle crack initiation. The numerous challenges with producing suitable welds of high quality are explained in this section. Due to the large thickness of the specimens, magnetism was introduced in the specimen during the machining and welding processes. The magnetism caused the weld to be uneven due to arc blow or arc wander[28]. This was combatted through a combination of surface peening and careful welding technique. Before welding, the entire specimen was surface peened using a 2 lb ball hammer with a focus around the bottom of the slot where the weld would be laid. The manual metal arc welding technique was used to deposit a brittle weld bead at the bottom of the slot for each specimen using the hard-facing electrode Bohler FoxDur 350 with a heat input of about 1.5 kJ/mm. The weld was notched to 2 mm depth using the EDM technique to introduce a starter notch in the test specimens.

There were challenges with ensuring a sufficient thickness of the weld deposit as it was necessary to complete the weld in a single pass. It was also necessary to increase the heat input from that recommended in the standard (from 1 kJ/mm to 1.5 kJ/mm) to ensure the weld deposit was thick enough to be notched. Some of the specimens which had poor quality of welds were re-welded by initially using EDM to remove the old weld deposit before introducing the weld bead again. Although this gives a concern that the excess heat input may affect the test results, this was localised to the crack initiation region; hence this process is believed not to have affected the bulk of the specimen where the crack is propagating and, most importantly the arresting region, which is further away from the initial crack tip. Through an iterative welding process, the deposition of the weld beads on test specimens was finalised. An example of a test specimen with the weld bead, before performing the test, is shown in Fig. 2.

4.1. Test procedure

According to the experimental approach detailed in the ASTM E1221 standard, side-grooved CCA specimens are slowly cyclically loaded under crack-line wedge loading to incrementally increasing peak loads, in order to achieve a rapid run-arrest of a crack with a nearly straight crack front. The temperature range for the CCA testing was chosen based on the ductile to brittle transition behaviour of the material, with the NDTT (−50 °C) chosen as the initial test temperature and subsequent temperatures chosen iteratively. In order to perform CCA experiments, the sample was initially cooled down to the desired test temperature using liquid nitrogen, and subsequently loaded and unloaded repeatedly to a higher load point in each cycle. This loading and unloading sequence continued until a brittle crack initiated and arrested itself. This was evident through the loud noise it made and also a steep drop-off in the load reading as the crack jumped. Once the experiment was completed, the specimens were heat tinted to highlight the notch and arrested crack clearly on the fracture surface once the specimen was broken open, so that the arrested crack length could be measured. The arrested crack length was measured as the average of three points equally distributed across the thickness of the specimen, as suggested by the ASTM E1221 standard[6].

To facilitate the experiments, a bespoke test rig was designed and fabricated at TWI Ltd., UK, using high strength steel based on the design suggested in the ASTM E1221 standard[6], which is shown in Fig. 3. The test rig included cooling coils embedded into the support block through which liquid nitrogen was pumped to ensure a consistent temperature throughout the specimen. Due to the large thickness of the material being tested, the whole rig was scaled up, including the wedge and split pin assembly, to ensure sufficient strength in the test rig. This was directly scaled from the example dimensions which are given in the standard.

Each stage of the experimental set-up is shown in Fig. 3. Fig. 3-a shows the test rig, which is fully set up on TWI's 500kN capacity machine in Fig. 3-b. The specimen was inserted into the test rig and

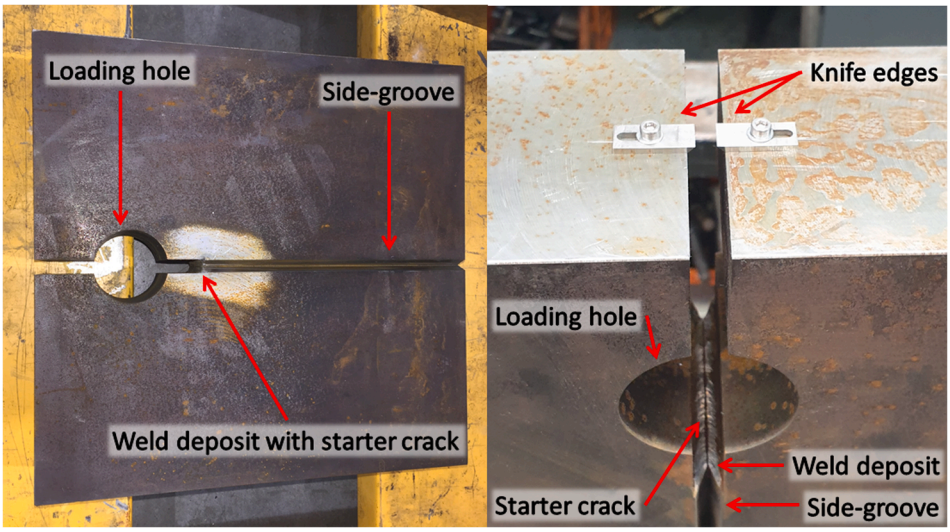

Fig. 2. Example of CCA specimen showing the weld bead and machined starter crack.

instrumented as shown in Fig. 3-c. The instrumentation included temperature measurements for all specimens and crack propagation monitoring wires which were used to measure the crack speed in two of the experiments. The case shown in Fig. 3-c is that with crack propagation monitoring wires applied to the surface of the specimen. As the crack propagates past the wire, it is broken and the signal is recorded and its speed can be measured. During the experiment, the low temperature was maintained by covering the specimen in thick layers of insulation, which is shown in Fig. 3-d.

4.2. Data analysis procedure

Eqs. (1)–(5) are used to calculate the stress intensity factor, *K*, shortly after arrest, which would be equivalent to K_{Ia} when particular requirements are met, as described by Eqs. (6)–(10). In order to perform a CCA test, the wedge is loaded cyclically into the specimen with increasing peak load, and the CMOD is used to find *K* once an arrest event has occurred. According to the ASTM standard, the stress intensity factor for standard CCA specimen geometry can be calculated using Eqs. (1)–(5):

$$K = E\delta Y\sqrt{\frac{B}{B_N W}} \tag{1}$$

$$Y = (1-x)^{\frac{1}{2}}(0.748 - 2.176x + 3.56x^2 - 2.55x^3 + 0.62x^4) \tag{2}$$

$$x = \frac{a}{W} \tag{3}$$

where E is the elastic Young's modulus in MPa, B is the specimen thickness in mm, B_N is the net thickness between the side grooves in mm, W is the specimen width in mm, δ is calculated from the CMOD using Equation (4) or Equation (5), and a is the crack length in mm (i.e. a_0 is the initial crack length and a_a is the arrested crack length). In order to calculate K_0, which is the stress intensity factor at initiation point (known as crack initiation toughness), the crack length is taken as $a = a_0$, and $\delta = d_0$. Similarly, K_a which is known as the crack arrest toughness is calculated using $a = a_a$ and $\delta = d_a$.

δ, used in Equation 1, is calculated from the equations below using Fig. 4 as a reference to show how the parameters are calculated from the load–displacement curve over multiple cycles.

$$d_0 = \delta_0 - (\delta_p)_{n-1} \tag{4}$$

$$d_a = 0.5\left[\delta_0 + \delta_a - (\delta_p)_1 - (\delta_p)_{n-1}\right] \tag{5}$$

where n is the number of load cycles to the run-arrest event, δ_0 is the CMOD at the crack initiation point, $\delta_{p(n-1)}$ is the CMOD at the start of the nth loading cycle when the load has been reset to 0, and δ_a is the CMOD after the crack has arrested. It can be seen that as the crack propagates, the crack mouth widens before it arrests.

According to ASTM E1221, when the following criteria are met K_a can be taken as K_{Ia} which is the critical stress intensity factor for crack arrest under the mode I fracture mechanics loading condition.

$$W - a_a \geq 0.15W \tag{6}$$

$$W - a_a \geq 1.25\left(\frac{K_a}{\sigma_{Yd}}\right)^2 \tag{7}$$

$$B \geq 1.0\left(\frac{K_a}{\sigma_{Yd}}\right)^2 \tag{8}$$

$$a_a - a_0 \geq 2N \tag{9}$$

$$a_a - a_0 \geq \left(\frac{K_0}{\sigma_{Ys}}\right)^2 /2\pi \tag{10}$$

where N is the machined slot width, W-a is the uncracked ligament, σ_{Yd} is the dynamic yield stress and σ_{Ys} is the static yield stress. These criteria ensure that the specimen is of a sufficiently large size to satisfy plane strain conditions, and that the assumption of static behaviour during the crack jump event is appropriate, i.e. dynamic effects are not present.

4.3. Small-scale testing

Following previous research conducted by the authors[26], where small-scale testing was carried out, the predictions of the crack arrest toughness obtained from smaller size samples were validated against the large-scale results presented in this study. The small-scale tests in the previous study consisted of instrumented Charpy V notch testing to determine the post-fracture force during impact, and drop weight Pellini testing to measure the NDTT. These predictions rely on the determination of reference temperatures and are based on the principles of the master curve approach. The master curve is a statistical approach which gives a lower bound estimate of fracture toughness of ferritic steels for temperatures in the transition region and lower shelf from a limited amount of test data. This has been adapted by other researchers [25,29–32] to predict brittle crack arrest toughness from small-scale testing using the following relationships:

Fig. 3. Experimental set up of CCA tests showing: (a) the test rig assembly, (b) the fully assembled test rig on the machine, (c) the specimen is placed in the test rig and instrumented, (d) during the test.

$$K_{Ia} = 49.957 + 16.878e^{0.028738(T-NDTT)} \text{[Ref32]} \quad (11)$$

$$K_{Ia} = 30 + 70e^{\left(\frac{T-T_{4kN}-12.3}{52.63}\right)} \text{[Ref30]} \quad (12)$$

where T is the calculation temperature, NDTT is measured from Pellini testing[33], and T_{4kN} is the temperature at which the instrumented Charpy post-fracture force is 4kN. These curves can be compared to the fit to the CCA data, which uses T_{KIa} as the reference temperature and is given in ASTM E1221[6] by:

$$K_{Ia(median)} = 30 + 70e^{0.019(T-T_{KIa})} \quad (13)$$

where T_{KIa} is the temperature corresponding to a median crack arrest toughness of 100 MPam$^{1/2}$.

5. Compact crack arrest test results

5.1. Validity of the test results

The results obtained from the CCA tests are summarised in Table 3 and compared against the predictions from small-scale testing in Fig. 5. While CCA2, CCA3, CCA4 and CCA8 specimens were tested satisfactorily according to ASTM E1221 and accurate crack arrest results were obtained from these four specimens, the remaining four samples resulted only in indicative crack arrest data as they were not fully qualified, due to a number of different reasons.

In the test on the CCA1 specimen, which was the first experiment conducted in this study, it was discovered that part of the loading rig had deformed during the loading of the specimen. This meant that the load recorded during the experiment was higher than the load applied onto the specimen, as some was lost to the loading rig. This did not affect the calculated crack arrest toughness as the load is not used as an input parameter into the calculation and the CMOD measurement was not

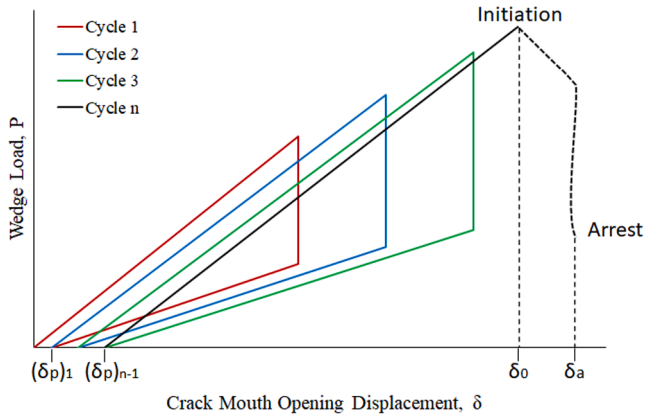

Fig. 4. Wedge force vs. CMOD using cyclic loading technique. Each loading cycle is shown in a different colour until the final "cycle n" where the crack propagates and arrests.

Table 3
Summary of the CCA test results.

Specimen ID	Temperature (°C)	Average arrested crack length, a_a (mm)	K_{Ia} (MPam^{½})
CCA1	−50	180.0	93.4
CCA2	−50	141.7	123.9
CCA3	−90	159.4	73.7
CCA4	−70	161.8	89.0
CCA5	−10	85.0	145.9
CCA6	−70	113.1	110.4
CCA7	−50	137.1	130.4
CCA8	−30	129.3	99.4

affected. Although this issue was unlikely to have impacted the results, the test data obtained from this experiment was assumed to be indicative. The issue with the loading rig was fixed after this first test and this problem did not occur again in any of the other tests.

In the test on the CCA5 specimen, the crack did not propagate through the entire thickness of the test geometry, presumably due to the comparatively high temperature in this specimen, which meant that the crack was arrested easily in the material. Therefore, the results obtained from this experiment were considered to be indicative. Finally, CCA6 and CCA7 test specimens were side-grooved in a single side, to be able to accommodate wiring on the opposite plane side of the test piece for measurement of the crack propagation speed. Although this was taken into account during the calculation of K_{Ia}, which includes consideration for the thickness between the side-grooves, the results obtained from these two test specimens were also considered indicative rather than strictly qualified to the standard.

5.2. Presentation of the test results

It is evident from Fig. 5 that there is a large scatter in the toughness results, and that not all of the test data points are valid. However, it can also be seen that both valid and indicative test data follow the same trend when the toughness data are correlated with the arrest temperature. Also seen in Fig. 5 is that the data points obtained from the CCA tests are entirely bounded by the two prediction lines which were made from small-scale testing. The prediction of the crack arrest toughness from NDTT gives a lower bound estimate, and the prediction from T_{4kN} gives an upper bound estimate with the CCA test data falling in between these two extreme trends. Also seen in Fig. 5 is that when the trend obtained from the test data points from this study is extrapolated to higher toughness values, the CCA trend remains between the prediction lines from NDTT and T_{4kN}. This suggests that the NDTT can be used to give a conservative estimate of CCA toughness results. However, more tests need to be conducted in future work to confirm the obtained trend from this study for higher and lower toughness values.

5.3. Fractography

Fractography analysis was carried out on all specimens post-testing. The fracture surfaces of one half of specimens CCA1–8 are shown in Fig. 6. It can be seen on the fracture surface of all specimens that heat tinting was an effective approach to mark the extent of crack growth during testing and before the specimen was broken open. The crack propagation occurred in a brittle manner in all specimens, which is evident from the relatively smooth and flat crack path observed in the fractography analysis on all test specimens. In specimens CCA6 and CCA7 (Fig. 6(f) and Fig. 6(g)), the crack showed tunnelling away from the surface, which meant that the crack propagation monitoring wires

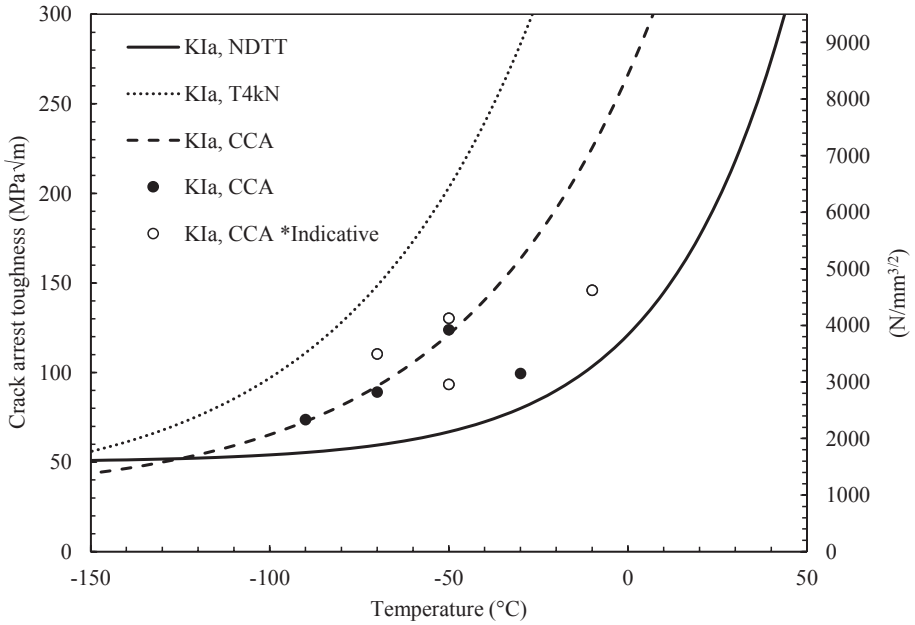

Fig. 5. Comparison of the CCA test results with predictions from small-scale testing.

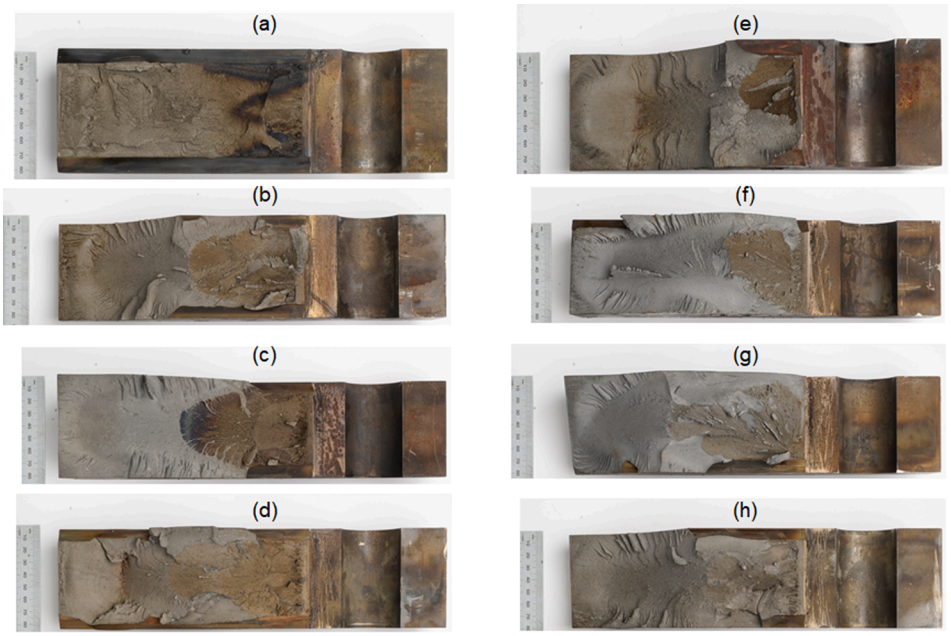

Fig. 6. Fracture surface of (a) CCA1, (b) CCA2, (c) CCA3, (d) CCA4, (e), CCA5 (f), CCA6 (g), CCA7, (h) CCA8 specimens.

were not broken as the crack propagated. This indicates that although these two specimens were instrumented for crack speed measurement, this could not be achieved in practice due to the lack of crack growth along the plane-sided face of the CCA specimen geometry.

6. Discussion

It was not possible to measure the crack velocity from these specimens. Due to the very low test temperatures (between −10 °C and −90 °C) it was necessary to keep the specimen under insulation which meant that it was not possible to use visual crack speed measurement methods (e.g. digital image correlation). For that reason, use of crack propagation monitoring wires is the recommended approach to measuring the crack speed. The focus of this research was on measurement of crack arrest toughness and ensuring that it was possible to obtain valid results before attempting to measure the crack speed, hence only two specimens were instrumented in this way. Now that the compact crack arrest testing approach has been proven successful, future work should focus on ensuring that the crack speed can be measured during these tests.

It is important to measure the crack propagation speed throughout the test as this is an important input into finite element modelling of brittle crack arrest which has been successfully carried out by other researchers [34–44]. The most common technique for finite element modelling of brittle crack arrest is using the nodal release method to replicate the propagating crack and extract the stress shortly ahead of the crack tip[39–41,45]. The critical stress just ahead of the crack tip is taken as the criterion for crack propagation, following a local stress approach[34,46]. Using this critical stress, predictive models can be developed. In future work, finite element modelling will be performed and validated using the experimental results.

The CCA results obtained from this study can be compared to those of other researchers who have carried out quantitative crack arrest testing on the same material. Although these experiments have never been done before on such thick sections of shipbuilding steels, other wide-plate tests have been carried out in previous studies using different methods [14]. Other researchers have consistently shown crack arrest toughness exceeding 6000 N/mm$^{3/2}$ at −10 °C (which is equivalent to 190 MPam^{½}) and this has been incorporated as a requirement of the International Association of Classification Societies[16,47,48]. Comparison of the results available on wide-plates with those obtained from CCA specimen geometries from the present study reveals that other test methods give a much higher threshold of brittle crack arrest toughness for the material examined in this study. This raises concerns that the CCA method may under-predict brittle crack arrest toughness results. Given the high strength and Charpy toughness of this material, it seems likely that it is the test method which is resulting in a low prediction of crack arrest toughness rather than the material itself. It would be necessary to carry out CCA testing and wide-plate testing on the same batch of steel in future work to have confidence in the agreement between the results of these two test methods. Alternatively, it may be possible to apply a correction factor to relate the CCA test results to wide-plate results for integrity assessment of large-scale structures. Last but not least, the presented results from this study will not be only of great interest to the shipbuilding industry but can be also employed in structural integrity assessment of other large-scale structures such as offshore wind turbine foundations [49–59].

7. Conclusions

CCA testing was successfully carried out on 80 mm thick EH47 shipbuilding steel to measure the brittle crack arrest toughness in this material. The results obtained from these tests were compared to the toughness predictions from small-scale testing and also wide-plate test results available from other researchers. The following conclusions were drawn from this study:

- The present study has proved the possibility of achieving valid results from CCA testing on relatively thick (i.e. 80 mm) steel plates
- The results show that Pellini NDTT data from small-scale tests can be used to obtain a conservative estimate of CCA test results
- The results show that instrumented Charpy testing provides an overestimation of the CCA test results
- Relatively smooth arrested fracture surfaces were observed in all CCA test specimens confirming that brittle crack arrest occurred in these experiments
- The wide-plate test results available in the literature on the EH47 steel indicate that more conservative values of brittle crack arrest toughness may be achieved from CCA tests

- More experiments should be conducted in future work on the same material batch to directly compare the CCA and wide-plate tests
- Crack speed monitoring in CCA tests is challenging and may not be achieved by instrumenting a plane sided face of the specimen

CRediT authorship contribution statement

Jessica Taylor: Conceptualization, Methodology, Formal analysis, Writing - original draft. **Ali Mehmanparast:** Supervision, Writing - review & editing. **Rob Kulka:** Writing - review & editing. **Philippa Moore:** Writing - review & editing. **Gholam Hossein Farrahi:** Writing - review & editing. **Li Xu:** Writing - review & editing.

Declaration of Competing Interest

The authors declare that they have no known competing financial interests or personal relationships that could have appeared to influence the work reported in this paper.

Acknowledgements

The authors would like to thank Lloyd's Register who kindly provided the EH47 shipbuilding steel used in this work and to Weihong He who arranged this. Thanks to TWI Ltd for provision of labs and technician support for the welding, mechanical testing and metallurgical investigation. This work was supported by Industrial CASE grant EP/P510464/1 (reference 2002942) and grant EP/L016303/1 for Cranfield, Oxford and Strathclyde Universities, Centre for Doctoral Training in Renewable Energy Marine Structures - REMS (http://www.rems-cdt.ac.uk/), both from the UK Engineering and Physical Sciences Research Council (EPSRC).

This publication was made possible by the sponsorship and support of Lloyd's Register Foundation. The work was enabled through, and undertaken at, the National Structural Integrity Research Centre (NSIRC), a postgraduate engineering facility for industry-led research into structural integrity established and managed by TWI through a network of both national and international Universities. Lloyd's Register Foundation helps to protect life and property by supporting engineering-related education, public engagement and the application of research.

References

[1] C.J. Tassava, Weak seams: Controversy over welding theory and practice in American shipyards, 1938–1946, Hist Technol. 19 (2) (2010) 87–108.
[2] International Association of Classification Societies. Safer and Cleaner Shipping - IACS. http://www.iacs.org.uk/.
[3] (DNV) Det Norske Veritas. Fatigue Design of Offshore Steel Structures, Recomm Pract DNV-RPC203. Published online 2005.
[4] S.E. Hirdaris, W. Bai, D. Dessi, et al., Loads for use in the design of ships and offshore structures, Ocean Eng. Published online (2014), https://doi.org/10.1016/j.oceaneng.2013.09.012.
[5] T.L. Anderson, Fracture Mechanics: Fundamentals and Applications 58 (2012). doi:10.1016/j.jmps.2010.02.008.
[6] ASTM. E1221 Standard Test Method for Determining Plane-Strain Crack-Arrest Fracture Toughness, K Ia, of Ferritic Steels. 2007;96(Reapproved):1-19. doi:10.1520/E1221-12A.2.
[7] K. Shibanuma, F. Yanagimoto, T. Namegawa, K. Suzuki, S. Aihara, Modeling of Brittle Crack Propagation / Arrest Behavior in Steel Plates, Procedia Struct. Integr. 2 (2016) 2598–2605, https://doi.org/10.1016/j.prostr.2016.06.325.
[8] T. Handa, T. Matsumoto, H. Yajima, et al., Effect of Structural Discontinuities of Welded Joints on Brittle Crack Propagation Behavior - Brittle Crack Arrest Design for Large Container Ships -3 - Steel Plates Used for Tests. 7 (2010) 88–94.
[9] T. Kawabata, K. Matsumoto, T. Ando, et al. Development of Brittle Crack Arrest Toughness Kca Test Method - Brittle Crack Arrest Design for Large Container Ships -2 - Review of Wide Plate Test Method for Arrest Toughness. 7 (2010) 80–87.
[10] Y. Funatsu, H. Shirahata, J. Otani, T. Inoue, Y. Hashiba, The Effect of Shear-lips on the Arrestability of Thicker Steel Plates Longitudinal, Isope. 4 (2012) 63–66.
[11] T. Kawabata, T. Namegawa, M. Kaneko, et al., Numerical analyses of press-notched bend tests and applicability to simplified method of arrest toughness evaluation, Proc Int Offshore Polar Eng Conf. 2015-Jan (2015) 169–176.
[12] T. Handa, S. Igi, K. Oi, et al., Effect of toughness distribution in the thickness direction on long brittle crack propagation/arrest behaviour of heavy gauge shipbuilding steel, Weld Int. 32 (7) (2018) 460–468, https://doi.org/10.1080/01431161.2017.1346884.
[13] T. Handa, T. Tagawa, F. Minami, Correlation between charpy transition temperature and brittle crack arrest temperature considering texture, Tetsu-To-Hagane/Journal Iron Steel Inst Japan. 98 (1) (2012) 32–38, https://doi.org/10.2355/tetsutohagane.98.32.
[14] T. Kawabata, T. Inoue, T. Tagawa, et al., Historical review of research on brittle crack propagation arresting technology for large welded steel structures developed in Japan with the application of Kca parameters, Mar. Struct. 71 (January) (2020), 102737, https://doi.org/10.1016/j.marstruc.2020.102737.
[15] S. Aihara, Y. Watabe, K. Shibanuma, T. Inoue, T. Koseki, Numerical and Experimental Analysis of Brittle Crack Propagation and Arrest in Steels. 4 (2012) 90–97.
[16] K. Shibanuma, F. Yanagimoto, T. Namegawa, K. Suzuki, Brittle crack propagation / arrest behavior in steel plate – Part II: Experiments and model validation, Eng. Fract. Mech. 162 (2016) 341–360, https://doi.org/10.1016/j.engfracmech.2016.02.053.
[17] G.B. An, J.S. Park, K.M. Ryu, et al. Brittle Crack Arrest Technique of Thick Steel Plate Welds in Container Ship, 1 (2009) 357–360.
[18] International Standards Organisation, BS ISO 20064 : 2019 BSI Standards Publication Metallic Materials — Steel — Method of Test for the Determination of Brittle Crack Arrest Toughness, K Ca., 2019.
[19] C. Wiesner, B. Hayes, A Review of Crack Arrest Tests, Models and Applications, 1995.
[20] I. Burch, J. Underwood, Crack Arrest Fracture Toughness Measurement of a Quenched and Tempered Ship Plate Steel, MRL Tech Rep. Published online 1992. http://www.dtic.mil/dtic/tr/fulltext/u2/a264037.pdf.
[21] E.D. Une, M. En, V.U.E.D.E. La, et al., Collection de notes internes de la Direction des Etudes et Recherches I, Practice.
[22] R.J. Bonenberger, J.W. Dally, On improvements in measuring crack arrest toughness, Int. J. Solids Struct. 32 (6–7) (1995) 897–909, https://doi.org/10.1016/0020-7683(94)00167-U.
[23] U. Mayer, A. Mutz, G. Ag, T. Nicak, Compact crack arrest tests for the validation of a finite element material model of the reactor pressure vessel steel of the nuclear power plant kkg, in: Proc ASME 2018 Press Vessel Pip Conf PVP2018. Published online 2018:PVP2018-84068.
[24] Ship Structures Committee, Crack Arrest Toughness of Steel Weldments, 2000.
[25] B.R. Bass, P.T. Williams, C.E. Pugh, An updated correlation for crack-arrest fracture toughness for nuclear reactor pressure vessel steels, Int. J. Press. Vessel. Pip. 82 (6) (2005) 489–495, https://doi.org/10.1016/j.ijpvp.2004.12.006.
[26] J. Taylor, A. Mehmanparast, R. Kulka, P. Moore, L. Xu, Farrahi G. Hossein, Experimental study of the relationship between fracture initiation toughness and brittle crack arrest toughness predicted from small-scale testing, Theor. Appl. Fract. Mech. 110 (October) (2020), 102799, https://doi.org/10.1016/j.tafmec.2020.102799.
[27] G.B. An, K.M. Ryu, J.S. Park, et al., Increase of Brittle Crack Arrestability Using Arrest Welding of Thick Steel Plate in Large Container Ship. 8 (2011) 2006–2009.
[28] B.J. Moniz, R.T. Miller, Welding Skills, American Technical Publishers, 2010.
[29] K. Wallin, Application of the Master Curve method to crack initiation and crack arrest, in: American Society of Mechanical Engineers, Pressure Vessels and Piping Division (Publication) PVP. Vol. 393, 1999.
[30] K. Wallin, P. Karjalainen-roikonen, Crack Arrest Toughness Estimation for High Strength Steels from Sub-Sized Instrumented Charpy-V Tests, Proc Twenty-sixth Int Ocean Polar Eng Conf. Published online (2016) 85–91.
[31] M.T. Kirk, M.E. Natishan, M. Wagenhofer, et al., A Summary of Wallin's Empirical Findings, Published online (2002) 729–740.
[32] C.E. Pugh, W.R. Corwin, S. Rhbryanbrbas, C.e. pugh, w.r. corwin, r.h, Nucl. Eng. Des. 96 (1986) 297–312.
[33] ASTM, E208 Standard Test Method for Conducting Drop-Weight Test to Determine Nil-Ductility Transition Temperature of Ferritic Steels 1. Test. 06(Reapproved) (2000) 1–13. doi:10.1520/E0208-06R12.2.
[34] K. Ishihara, T. Hamada, N. Kikuya, T. Meshii, Applicability Of Modified Ritchie-Knott-Rice Failure Criterion To Predict The Onset Of Cleavage Fracture For The Test Specimen With Residual Stress Introduced To The Crack Tip, Procedia Struct Integr. 2 (2016) 728–735, https://doi.org/10.1016/j.prostr.2016.06.094.
[35] B. Prabel, S. Marie, A. Combescure, Using the X-FEM method to model the dynamic propagation and arrest of cleavage cracks in ferritic steel. 75 (2008) 2984–3009. doi:10.1016/j.engfracmech.2008.01.008.
[36] A. Bousquet, S. Marie, P. Bompard, Propagation and arrest of cleavage cracks in a nuclear pressure vessel steel, Comput. Mater. Sci. 64 (2012) 17–21, https://doi.org/10.1016/j.commatsci.2012.04.026.
[37] C. Berdin, M. Hajjaj, P. Bompard, S. Bugat, Local approach to fracture for cleavage crack arrest prediction, Eng. Fract. Mech. 75 (2008) 3264–3275.
[38] A. Dahl, C. Berdin, D. Moinereau, Dynamic modeling of cleavage crack propagation and arrest with a local approach, Procedia Eng. 10 (2011) 1853–1858, https://doi.org/10.1016/j.proeng.2011.04.308.
[39] C. Berdin, 3D modeling of cleavage crack arrest with a stress criterion, Eng Fract Mech. 90 (2012) 161–171, https://doi.org/10.1016/j.engfracmech.2012.05.002.
[40] Y. Nishioka, K. Shibanuma, Y. Nishioka, F. Yanagimoto, Finite element model to simulate crack propagation based on local fracture stress criterion. Published online 2016.
[41] F. Yanagimoto, K. Shibanuma, K. Suzuki, T. Matsumoto, S. Aihara, Local stress in the vicinity of the propagating cleavage crack tip in ferritic steel, Mater. Des. 144 (2018) 361–373.
[42] F. Yanagimoto, K. Shibanuma, K. Suzuki, T. Matsumoto, A physics based model to simulate brittle crack arrest in steel plates incorporating experimental and

numerical evidences, Eng. Fract. Mech. 221 (January) (2019), 106660, https://doi.org/10.1016/j.engfracmech.2019.106660.
[43] K. Shibanuma, F. Yanagimoto, T. Namegawa, K. Suzuki, Brittle crack propagation / arrest behavior in steel plate – Part I: Model formulation, Eng. Fract. Mech. 162 (2016) 324–340, https://doi.org/10.1016/j.engfracmech.2016.02.054.
[44] R.E. Link, J.A. Joyce, C. Roe, Crack arrest testing of high strength structural steels for naval applications q, Eng. Fract. Mech. 76 (3) (2009) 402–418, https://doi.org/10.1016/j.engfracmech.2008.11.006.
[45] R. Link, Analysis of Dynamic Fracture and Crack Arrest of an HSLA Steel in an SE (T) Specimen. 3(1) (2006) 1–26.
[46] R.O. Ritchie, J.F. Knott, J.R. Rice, On the relationship between critical tensile stress and fracture toughness in mild steel, J. Mech. Phys. Solids. 21 (6) (1973) 395–410, https://doi.org/10.1016/0022-5096(73)90008-2.
[47] International Association of Classification Societies, W31 YP47 Steels and Brittle Crack Arrest Steels, 2019.
[48] G.B. An, K.M. Ryu, J.S. Park, et al. Increase of Fracture Toughness using Crack Arrest Design of Thick Steel Plate Welds in Large Container Ship. 7 (2010) 119–121.
[49] V. Igwemezie, A. Mehmanparast, F. Brennan, The role of microstructure in the corrosion-fatigue crack growth behaviour in structural steels, Mater. Sci. Eng.: A 803 (2021) 140470.
[50] V. Igwemezie, A.. Mehmanparast, F. Brennan, The influence of microstructure on the fatigue crack growth rate in marine steels in the Paris Region, Fatigue Fract. Eng. Mater. Struct. 43 (2020) 2416–2440.
[51] V.. Igwemezie, A. Mehmanparast, Waveform and Frequency Effects on Corrosion-Fatigue Crack Growth Behaviour in Modern Marine Steels, Int. J. Fatigue 134 (2020) 105484.
[52] V. Igwemezie, P. Dirisu, A. Mehmanparast, Critical assessment of the fatigue crack growth rate sensitivity to material microstructure in ferrite-pearlite steels in air and marine environment, Mater. Sci. Eng.: A 754 (2019) 750–765.
[53] V. Igwemezie, A. Mehmanparast, A. Kolios, Current trend in offshore wind energy sector and material requirements for fatigue resistance improvement in large wind turbine support structures–A review, Renew. Sustain. Energy Rev. 101 (2019) 181–196.
[54] V. Igwemezie, A. Mehmanparast, A. Kolios, Materials selection for XL wind turbine support structures: A corrosion-fatigue perspective, Mar. Struct. 61 (2018) 381–397.
[55] A. Jacob, J. Oliveira, A.. Mehmanparast, F.. Hosseinzadeh, J. Kelleher, F. Berto, Residual stress measurements in offshore wind monopile weldments using neutron diffraction technique and contour method, Theoret. Appl. Fract. Mech. 96 (2018) 418–427.
[56] A. Jacob, A. Mehmanparast, R. D'Urzo, J. Kelleher, Experimental and numerical investigation of residual stress effects on fatigue crack growth behaviour of S355 steel weldments, Int. J. Fatigue 128 (2019) 105196.
[57] A. Jacob, A. Mehmanparast, Crack growth direction effects on corrosion-fatigue behaviour of offshore wind turbine steel weldments, Mar. Struct. 75 (2021) 102881.
[58] A. Mehmanparast, J. Taylor, F. Brennan, I. Tavares, Experimental investigation of mechanical and fracture properties of offshore wind monopile weldments: SLIC interlaboratory test results, Fatigue Fract. Eng. Mater. Struct. 41 (12) (2018) 2485–2501.
[59] A.. Mehmanparast, F. Brennan, I. Tavares, Fatigue crack growth rates for offshore wind monopile weldments in air and seawater: SLIC inter-laboratory test results, Mater. Des. 114 (2017) 494–504.